NASA TM-8637

NASA Technical Memorandum 86376

NASA-TM-86376 19850012806

MEASURED UNSTEADY TRANSONIC AERODYNAMIC CHARACTERISTICS OF AN ELASTIC SUPERCRITICAL WING WITH AN OSCILLATING CONTROL SURFACE

DAVID A. SEIDEL, MAYNARD C. SANDFORD
AND CLINTON V. ECKSTROM

FEBRUARY 1985

National Aeronautics and
Space Administration

Langley Research Center
Hampton, Virginia 23665

MEASURED UNSTEADY TRANSONIC AERODYNAMIC CHARACTERISTICS OF AN ELASTIC SUPERCRITICAL WING WITH AN OSCILLATING CONTROL SURFACE

David A. Seidel, Maynard C. Sandford, and Clinton V. Eckstrom
NASA Langley Research Center
Hampton, Virginia 23665

Abstract

Transonic steady and unsteady aerodynamic data were measured on a large elastic wing in the NASA Langley Transonic Dynamics Tunnel. The wing had a supercritical airfoil shape and a leading-edge sweepback of 28.8°. The wing was heavily instrumented to measure both static and dynamic pressures and deflections. A hydraulically driven outboard control surface was oscillated to generate unsteady airloads on the wing. Representative results from the wind tunnel tests are presented and discussed, and the unexpected occurrence of an unusual dynamic wing instability, which was sensitive to angle of attack, is reported.

Nomenclature

C_p	pressure coefficient
f	frequency of oscillating control surface, Hertz
Hz	Hertz, cycles/second
M	free-stream Mach number
q	free-stream dynamic pressure, psf
x/c	chordwise location, fraction of local chord
α	wing root angle of attack, degrees (positive leading edge up)
δ_d	amplitude of control surface oscillation, degrees
δ_m	mean control surface deflection angle, degrees (positive leading edge up)
ΔC_p	lifting pressure coefficient (positive up)
η	spanwise location, fraction of semi-span

Introduction

For the past decade the NASA Langley Research Center has pursued a program of unsteady pressure measurements on essentially rigid wing models for the purpose of evaluating computational transonic aerodynamic codes, and three such models have been tested in the Transonic Dynamics Tunnel (TDT). These rigid large wing configurations included a clipped delta wing with a circular arc airfoil,[1] a high-aspect-ratio wing with a supercritical airfoil[2] and a rectangular wing with a supercritical airfoil.[3] All of these wings were made rigid to minimize dynamic structural effects and thereby simplify correlation with the computational results. Real airplane wings are elastic structures, however, and it is desirable to test an elastic wing model to assess the accuracy of transonic computer codes for predicting the aeroelastic response of wings, including flutter.

A delay in the NASA program, Drones for Aerodynamic and Structural Testing (DAST),[4] made the second Aeroelastic Research Wing, ARW-2, available for testing in the Langley TDT. This elastic wing configuration had a 10.3 aspect ratio, a leading-edge sweepback angle of 28.8° and a supercritical airfoil. The wing had a hydraulically driven outboard trailing-edge control surface and was instrumented with unsteady pressure gauges. The primary purpose of these tests was to obtain unsteady pressure measurements on an elastic wing. Secondary objectives were to provide an early assessment of the wing aeroelastic stability over a wide range of angles of attack and to provide wind tunnel data for comparison with planned flight test data.

This paper presents some representative results from the elastic wing tests in which the outboard control surface was used to generate unsteady pressures. Wind tunnel Mach numbers varied from 0.60 to 0.90 at dynamic pressures from less than 50 to over 300 pounds per square foot (psf). Model parameters investigated include wing angle of attack, control surface mean angle, and control surface oscillation amplitude and frequency.

Wind Tunnel Model

General

The elastic semi-span wing used in the present study is the DAST ARW-2 right wing panel. A half-body fuselage was used to simulate the drone fuselage. This fuselage had shorter nose and tail sections than does the drone fuselage since no supersonic tests were to be made. The center section of the fuselage was similar to the actual drone fuselage in both diameter and wing location to generate the proper airflow over the inboard section of the wing. Both the fuselage and the wing were mounted on a remotely controlled turntable mechanism located on the tunnel sidewall. Figure 1 shows the wing and fuselage configuration mounted in the wind tunnel.

Geometry

The wing planform and instrumentation locations are shown in Figure 2. The wing had an aspect ratio of 10.3 with a leading-edge sweep angle of 28.8°. The wing was equipped with three hydraulically driven control surfaces, two inboard and one outboard. The inboard surfaces were held fixed at 0° deflection and only the outboard surface was

deflected statically and dynamically. The outboard surface hinge line was located at 77 percent of local chord.

The wing contour was formed from three different supercritical airfoils. These three airfoils were located at the following spanwise wing stations: the wing-fuselage junction (η= 0.071), the wing planform break (η = 0.426) and the wing tip (η = 1.000) and had thickness-to-chord ratios of 0.15, 0.12 and 0.11, respectively. The three supercritical airfoil shapes and wing twist were defined for the design cruise condition and are described in ref. 5. Straight line interpolation along constant percent chords was used to define the wing contour between these three airfoil sections. The wing construction jig shape was then derived from the defined cruise shape, the corresponding loading conditions and the flexibility of the wing structure.

Instrumentation

The locations of the wing instrumentation are shown in Figure 2. The instrumentation consisted of 191 pressure transducers and 10 accelerometers. In addition, strain gauges were located near the wing root to measure bending moments. Differential pressure gauges were mounted in each supply line to the hydraulic actuators of each control surface to measure hinge moments. Small potentiometers were used to measure the control surface angular displacement. The model angle of attack was measured by a servo accelerometer that was mounted near the wing root. Both steady and unsteady pressures were obtained using differential pressure transducers referenced to the tunnel's static pressure. Streamwise rows of upper and lower surface pressure orifices were located at six span stations. The orifice rows were located at η = 0.274, 0.476, 0.599, 0.707, 0.871 and 0.972. The fifth row at η = 0.871 lies along the mid-span of the outboard control surface. All of these surface orifices were connected to pressure transducers by matched tubes having an inner diameter of 0.020 inch and a length of 18 inches. In order to determine the tube transfer functions needed to correct the unsteady pressure data from these matched-tube transducers, simultaneous measurements were also obtained from a row of in situ transducers mounted on the wing upper surface parallel to the fifth row of surface orifices. Dynamic wing deflections were determined using the 10 accelerometers.

Wind Tunnel

The Langley Transonic Dynamics Tunnel (TDT) is a closed-circuit continuous-flow tunnel which has a 16-foot square test section with slots in all four walls. Mach number and dynamic pressure can be varied simultaneously, or independently, with either air or Freon as a test medium. Freon was used for the majority of tests of the investigation.

Data Acquisition and Analysis

Data from the model instrumentation were acquired using the TDT real-time data acquisition system.[6] The pressure data were acquired using the electronically scanned pressure (ESP) system.[7] The ESP system is a sequential, digital pressure sampling system equivalent to a mechanical scani-valve. All data were digitized in real-time at 250 samples per second and written on magnetic tape for later analysis. Static pressures were measured by all 191 pressure transducers. Each pressure signal was averaged for 0.3 seconds to acquire its mean value.

Dynamic pressure time histories for the three outboard rows of surface orifices and accelerometer time histories were recorded for a minimum of 50 cycles of control surface oscillation. Discrete Fourier transforms of these time histories then provided the magnitude and phase angle at the frequency of the oscillating control surface for each transducer and accelerometer. All phase angles are relative to the position of the oscillating control surface.

Wing bending moments were measured for all cases where static pressures were recorded. The bending gauge measurements were averaged for 0.3 seconds to obtain a mean value for wing bending moment for each gauge.

The control surface static hinge moments were measured using two pressure gauges installed in each of the two hydraulic supply lines to the actuator.[2] The mean value of the differential pressure between the two gauges is directly related to the control surface hinge moment. To obtain quasi-steady hinge moments, the control surface was oscillated at a low frequency of 0.5 Hz and amplitude, δ_d, of 1° to eliminate the influence of high friction loads created by the internal seal of the actuator. The resulting differential signal was averaged for 10 seconds to acquire a mean value for the hinge moment.

Test Results and Discussion

Steady and unsteady pressures were measured for a large number of test conditions in the TDT using Freon as a test medium. The test conditions at which pressure data were taken is shown in Figure 3. Data were taken at Mach numbers of 0.6, 0.7, 0.8, 0.85 and 0.88 and at dynamic pressures of 100, 200 and 300 pounds per square foot (psf). At each tunnel condition static pressure data were taken for wing angles of attack of -2 to 4 degrees for the control surface undeflected (δ_m = 0°). Some of the high angle of attack values were eliminated at the higher dynamic pressures due to maximum bending moment restrictions imposed on the wing. For wing angles of attack of 0 and 2 degrees the control surface static deflection, δ_m, was varied from -8 to 8 degrees. Unsteady pressure data was taken at wing angles of attack of 0 and 2 degrees for control surface oscillation amplitudes of δ_d equal to 1, 2 and 3 degrees and frequencies of 5, 15 and 20 Hz.

Steady Pressure Results

Span Effects: Figure 4 shows the steady chordwise pressure distribution at the six span

stations near the design cruise condition ($M = 0.8$, $\alpha = 2°$, $q = 100$ psf and $\delta_m = 0°$). The data show that a shock is present on the upper surface of the wing and the shock location varies with span. The steady shock location, in terms of local chord, moves aft between 27 and 87 percent span then moves forward between 87 and 97 percent span.

Mach Number Effects: Figure 5 shows the steady pressure distributions at the 87 percent span station for five Mach numbers for 2° angle of attack, a dynamic pressure of 100 psf and an outboard mean control surface deflection, δ_m, of 0°. As Mach number increases, a shock can be seen to have formed near 30 percent chord at a Mach number equal to 0.80 and to move aft to about 70 percent chord at a Mach number equal to 0.88. Attached flow is indicated at all Mach numbers except at a Mach number of 0.88 where the pressure distribution indicates that there is flow separation on the upper surface near the trailing edge.

Angle of Attack Effects: The variation of the steady lifting pressure with angle of attack at Mach number of 0.80 and dynamic pressure of 100 psf is shown in Figure 6 for the 87 percent span station. The shock develops and moves aft as the angle of attack increases from -2 to 4 degrees.

Unsteady Pressure Results

Mach Number Effects: Figure 7 shows the variation of the unsteady lifting pressure distribution with Mach number at the 87 percent span station. The outboard control surface was oscillated with an amplitude $\delta_d = 1°$ about a mean deflection of $\delta_m = 0°$ at 15 Hz. The magnitude and phase components of the unsteady lifting pressure are plotted versus percent chord. For all Mach numbers a peak in the pressure magnitude occurs just forward of the control surface hinge line location. An additional peak in the magnitude can be seen to occur at the mean shock location for Mach numbers 0.70 to 0.85 (see Figure 5). This peak is probably caused by the shock motion generated by the oscillatory control surface motion. The mean shock location can be seen to move aft with increasing Mach number. The mean shock peak and control hinge line peak appear to merge at a Mach number of 0.85. The peak in the pressure magnitude near the control surface hinge line increases with increasing Mach number through Mach number of 0.85, but then drops to the lowest value at Mach number of 0.88. In addition, no mean shock peak can be seen in the pressure magnitude at a Mach number of 0.88. These phenomena may be attributable either to the flow separation which occurs in the trailing edge region of the wing at a Mach number of 0.88, or to the transducers being too far apart near the hinge line to show the existance of a peak.

Frequency Effects: Figure 8 shows the variation of the unsteady lifting pressure with oscillation frequency at the 87 percent span station. At the upper surface mean shock location the magnitude of the unsteady pressure increases with increasing frequency from 5 to 20 Hz except at 10 Hz. The magnitude peak for the 10 Hz oscillation is much greater than that for the other frequencies, probably because this 10 Hz frequency was very close to the wing first bending frequency of 8.3 Hz (wind-off).

Wing Deflections

For rigid wing pressure studies, the assumption is made that the wing does not deform, and therefore only the measured pressure distributions are needed. In contrast, for elastic wing pressure studies, the above assumption is not true. Therefore both the measured pressure distributions and the corresponding measured deformed wing shape are needed to define the aerodynamic loading characteristics for a given wing configuration.

In the present study a technique known as stereophotogrammetry was used to measure the static wing deflections.[8] Due to the large amount of labor required to read the photos and analyze the data, the stereophotogrammetry deflection results are not available at this time. However, during these tests some deflection measurements of the wing tip were made using a cathetometer instrument focused on a straight line drawn on the tip of the wing. Both vertical deflections and angular deflections of the wing tip were measured at selected test points. Illustrative results of these wing tip deflection measurements at a Mach number of 0.80 and an angle of attack of 0° are shown in Figure 9. The variation of the wing tip vertical deflection with dynamic pressure is presented in Figure 9(a) and the associated wing tip twist angle is presented in Figure 9(b). Clearly, the elastic wing exhibits significant nonlinear tip deflections, with vertical deflections of over 4 inches and a negative tip twist of over 3 degrees occurring at the higher dynamic pressures.

The present study used selectively spaced accelerometers mounted on the wing to obtain dynamic wing deflections for all wing tests of forced oscillatory motion. A discrete Fourier analysis was performed on each accelerometer signal at the known frequency of oscillation to obtain the amplitude of acceleration which was then integrated twice to obtain magnitude of the motion at the corresponding wing location.

Figure 10 shows the wing deflection mode shape derived from the accelerometer data for the cases shown in Figure 8. The vertical deflection at the elastic axis is plotted for four oscillation frequencies. The elastic axis is located midway between the accelerometers shown in Figure 2. As mentioned, at excitation frequencies near 10 Hz the coupling of the forcing function frequency with the wing's first bending mode caused large dynamic wing deflections. Testing at 10 Hz was therefore discontinued after tests at only a few wing and tunnel conditions.

Wing Instability

An unusual wing instability, similar to wing first bending motion, was encountered at the beginning of these tests. The occurrence of

the instability was surprising at the low dynamic pressures of about 100 pounds per square foot where it was first encountered at a Mach number of above 0.90. This instability generated much interest as to its character and the boundary was determined for a wing angle of attack of 0° within the wind tunnel limits as shown in Figure 11. Also, shown in Figure 11 as a solid line, is the predicted linear theory (doublet lattice) flutter boundary for comparison with the much lower dynamic pressures of the measured instability boundary. The measured boundary was determined using a familiar subcritical response technique known as peak-hold.[9] Although the peak-hold results show a definite indication of instability onset, hard instability (zero damping) points were avoided for fear of damaging the model and thereby risking both the unsteady pressure tests and the DAST flight test program. An exception to this policy was the very lowest dynamic pressure point on the boundary where a hard instability was obtained at a Mach number of 0.895 and with a slight increase in Mach number to 0.900 the wing became stable. This exercise was performed to establish that the test conditions at this point were at or near the boundary minimum. The boundary occurs at a nearly constant Mach number of 0.90 beginning at a low dynamic pressure of about 50 psf and rising near vertically to over 300 psf. At this time, no adequate explanation can be given for the higher Mach number variation in the boundary near 100 psf. The observed wing motion during the instability was similar to the wing first bending mode, the frequency of which was measured to be 8.3 Hz in the wind-off model vibration tests. The instability frequency was 8.6 Hz at the lowest dynamic pressure point and increased with dynamic pressure to about 13 Hz at the highest dynamic pressure point. It is interesting to note that the predicted flutter frequency was 24.3 Hz at a Mach number of 0.80.

Because of much recent interest in angle of attack effects and shock induced effects on wing instabilities,[10] several additional tests were made which included variation of the wing angle of attack as the boundary was approached, comparison of air and Freon instability boundaries and comparison of the boundaries with and without a transition strip near the wing leading edge. The instability was found to be sensitive to variation in angle of attack and, generally, the minimum damping occurred at or near zero angle of attack. In Figure 11 the solid symbol indicates the Mach number and dynamic pressure where the comparison tests were made. The results showed no significant difference in the instability boundary for tests in air or Freon. There were also no significant differences for tests in Freon with or without a transition strip.

Wing Bending Moments

Static wing bending moments were measured for a wide variety of conditions. For a given Mach number and dynamic pressure the wing bending moments were measured as the wing angle of attack was varied from -2 to 4 degrees. The result of these measurements for a Mach number of 0.80 is shown in Figure 12 where the bending moment variation with wing angle of attack is shown for several values of dynamic pressure. The bending moments essentially vary linearly with angle of attack, but are not linear with variations in dynamic pressure. This nonlinearity is due to the loss of lift at the wing tip resulting from the negative tip twist which occurred with increasing dynamic pressure as shown in Figure 9(b). The bending moment shows essentially no variation with dynamic pressure near -2.0° angle of attack.

Control Surface Hinge Moments

Measured static control surface hinge moments for a Mach number of 0.80 and zero angle of attack are presented in Figure 13. The results are shown in terms of hinge moment variation with control surface angle for several values of dynamic pressure. The overall results appear to be reasonably linear over the range of test parameters although some scatter in the data can be observed.

Concluding Remarks

Steady and unsteady pressures were measured on an elastic high aspect ratio supercritical wing. An outboard trailing-edge control surface was oscillated at various amplitudes and frequencies to obtain unsteady data. The data were acquired for a wide range of test conditions which included variations in Mach number from 0.60 to 0.90, dynamic pressure from less than 50 to over 300 psf, wing angle of attack from -2 to 4 degrees, control surface mean angle from -8 to 8 degrees and control surface oscillation amplitudes of 1, 2 and 3 degrees at frequencies of 5, 10, 15 and 20 Hz. Static and dynamic wing deflections were also measured. In addition, static wing bending moments and static control surface hinge moments were measured.

An unusual wing instability was found to exist in the wind tunnel at much lower dynamic pressure values than those of the predicted flutter boundary. This wing instability boundary was well defined and occurred at a nearly constant Mach number of about 0.90 and varied in dynamic pressure from below 50 psf to above 300 psf. The frequency of this wing instability ranged from about 8.6 Hz at the minimum dynamic pressure to about 13 Hz at the maximum dynamic pressure. The wing instability motion was dominated by the wing first bending mode which had a measured frequency of 8.3 Hz during the ground vibration tests. The instability was found to be sensitive to angle of attack, with minimum damping occurring near zero degrees. Comparison tests conducted in air and Freon showed no significant difference in the instability boundary. Tests in Freon with and without a transition strip also showed no significant differences.

References

[1]Hess, R. W.; Wynne, E. C.;; and Cazier, F. W., Jr.: Static and Unsteady Pressure Measurements on a 50 Degree Clipped Delta Wing at M = 0.9. NASA TM 83297, April 1982.

[2]Sandford, M. C.; Ricketts, R. H.; Cazier, F. W., Jr.; and Cunningham, H. J.: Transonic Unsteady Airloads on an Energy Efficient Transport Wing with Oscillating Control Surfaces. Journal of Aircraft, Vol. 18, No. 7, July 1981, pp. 557-561.

[3]Ricketts, R. H.; Sandford, M. C.; Seidel, D. A.; and Watson, J. J.: Transonic Pressure Distributions on a Rectangular Supercritical Wing Oscillating in Pitch. Journal of Aircraft, Vol. 21, No. 8, August 1984, pp. 576-582.

[4]Murrow, H. N.; and Eckstrom, C. V.: Drones for Aerodynamic and Structural Testing (DAST) - A Status Report. Journal of Aircraft, Vol. 16, No. 8, August 1979, pp. 521-526.

[5]Byrdsong, T. A.; and Cuyler, W. B., Jr.: Wind-Tunnel Investigation of Longitudinal and Lateral-Directional Stability and Control Characteristics of a 0.237-Scale Model of a Remotely Piloted Research Vehicle With a Thick, High-Aspect-Ratio Supercritical Wing. NASA TM 81790, July 1980.

[6]Cole, P. H.: Wind Tunnel Real-Time Data Acquisition System. NASA TM 80081, April 1979.

[7]Chapin, W. G.: Dynamic-Pressure Measurements Using an Electronically Scanned Pressure Module. NASA TM 84650, July 1983.

[8]Brooks, J. D.; and Beamish, J. K.: Measurement of Model Aeroelastic Deformations in the Wind Tunnel at Transonic Speeds Using Stereophotogrammetry. NASA TP 1010, October 1977.

[9]Sandford, M. C.; Abel, I.; and Gray, D. L.: Development and Demonstration of a Flutter-Suppression System Using Active Controls. NASA TR R-450, December 1975.

[10]Yates, E. C., Jr.; Wynne, E. C.; and Farmer, M. G.: Effects of Angle of Attack on Transonic Flutter of a Supercritical Wing. Journal of Aircraft, Vol. 20, No. 10, October 1983, pp. 841-847.

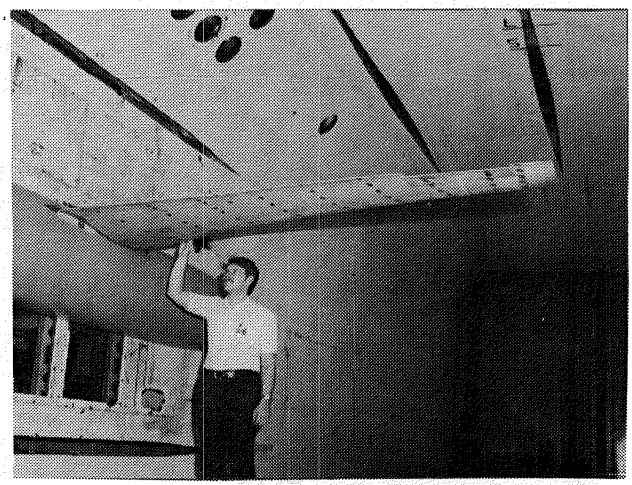

Fig. 1 Wing mounted in TDT test section.

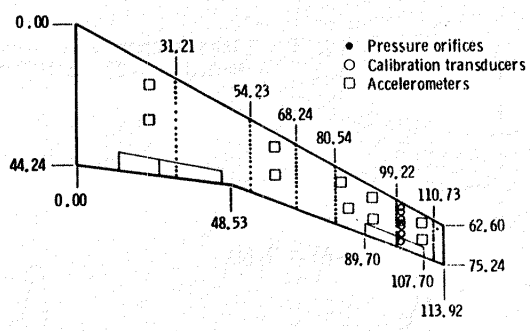

Fig. 2 Wing planform and instrumentation locations (in inches).

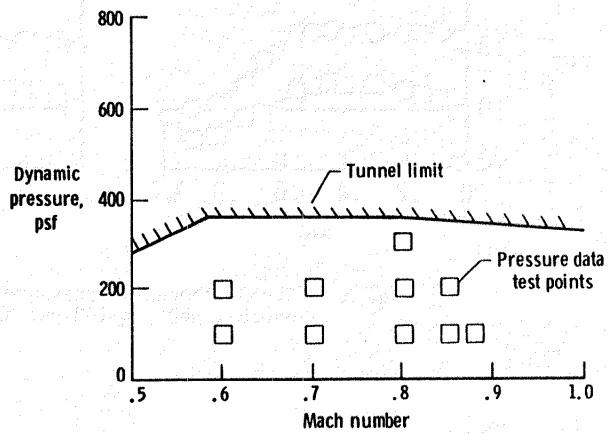

Fig. 3 Wind tunnel test conditions.

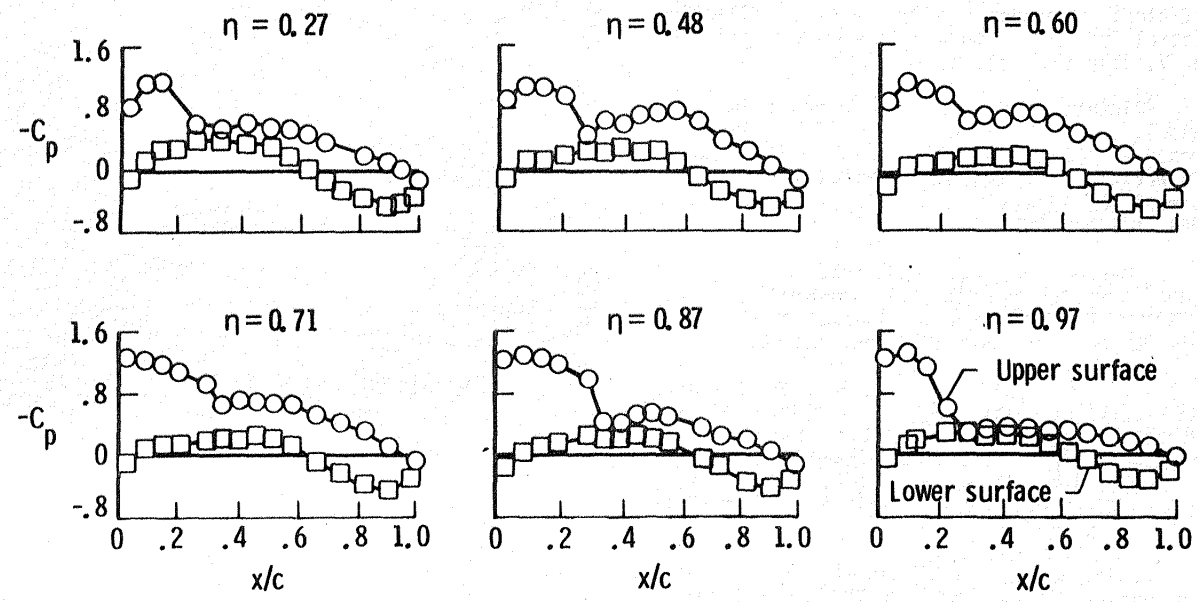

Fig. 4 Steady chordwise pressure distributions at six span stations; M=0.80, α=2°, q=100 psf and δ_m=0°.

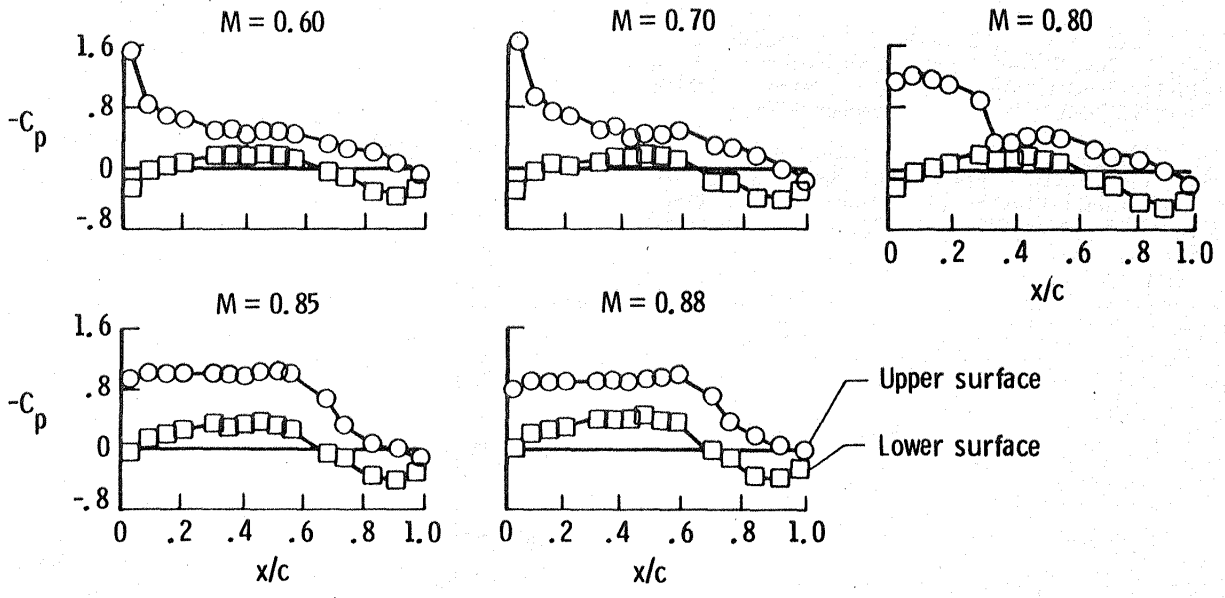

Fig. 5 Steady chordwise pressure distributions for five Mach numbers at η=0.87; α=2°, q=100 psf and δ_m=0°.

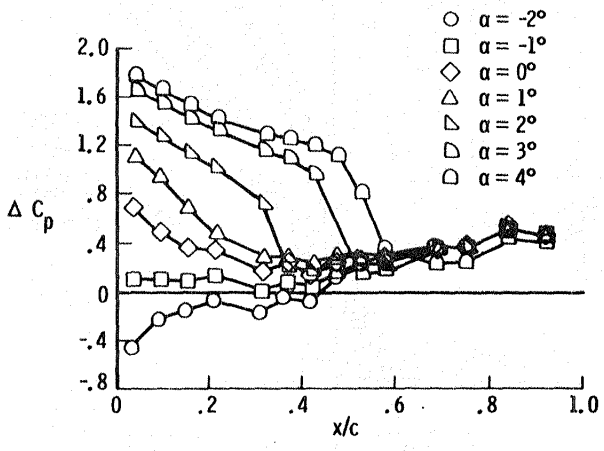

Fig. 6 Effect of angle of attack on steady lifting pressure distribution at η=0.87; M=0.80, q=100 psf and δ_m=0°.

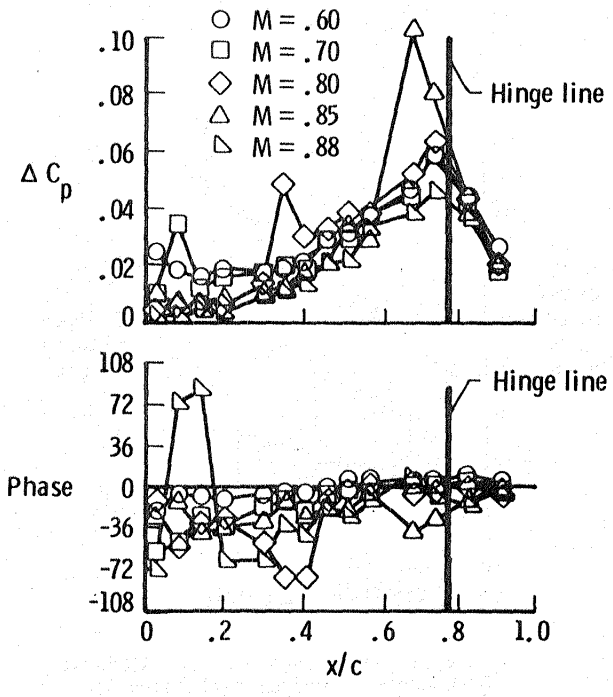

Fig. 7 Effect of Mach number on unsteady lifting pressure distribution at η=0.87; α=2°, q=100 psf, δ_m=0°, δ_d=1° and f=15 Hz.

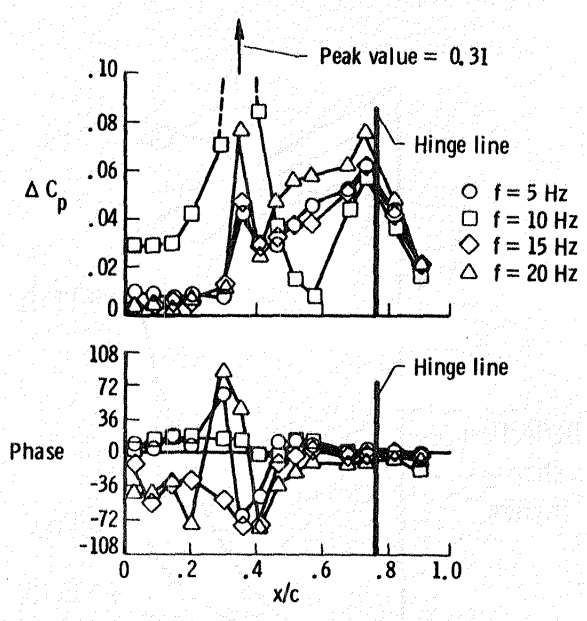

Fig. 8 Effect of frequency on unsteady lifting pressure distribution at η=0.87; M=0.80, α=2°, q=100 psf, δ_m=0° and δ_d=1°.

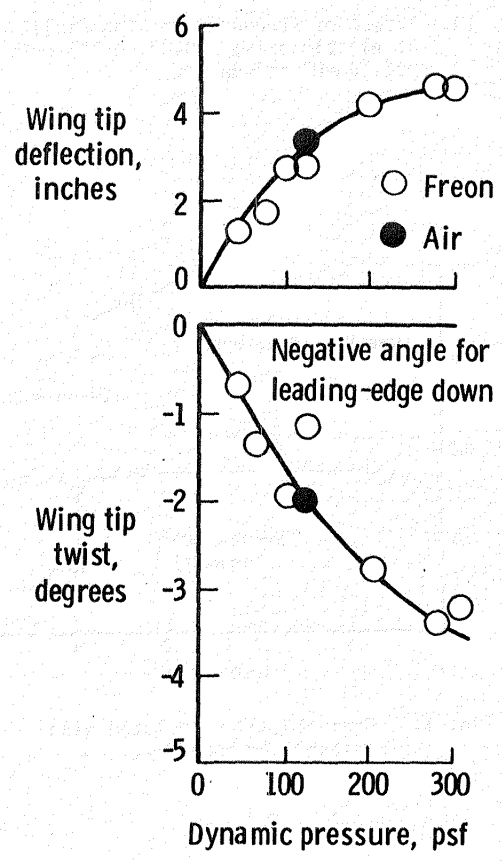

Fig. 9 Measured static wing tip deflections versus dynamic pressure; M=0.80 and α=0°.

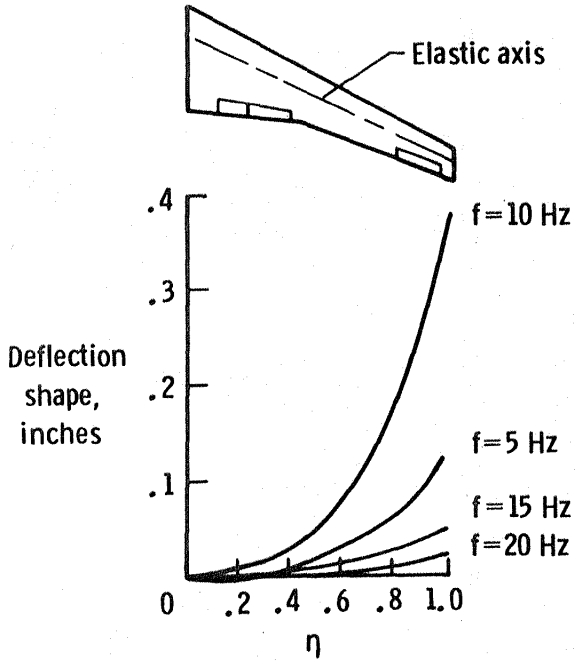

Fig. 10 Effect of frequency on wing amplitude at elastic axis; M=0.80, α=2°, q=100 psf, δ_m=0° and δ_d=1°.

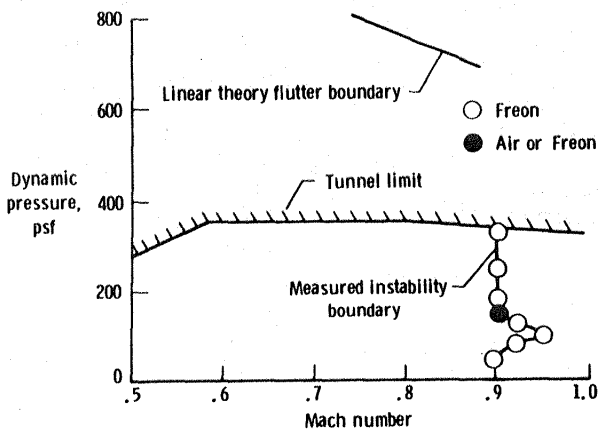

Fig. 11 Measured and calculated wing instability boundary.

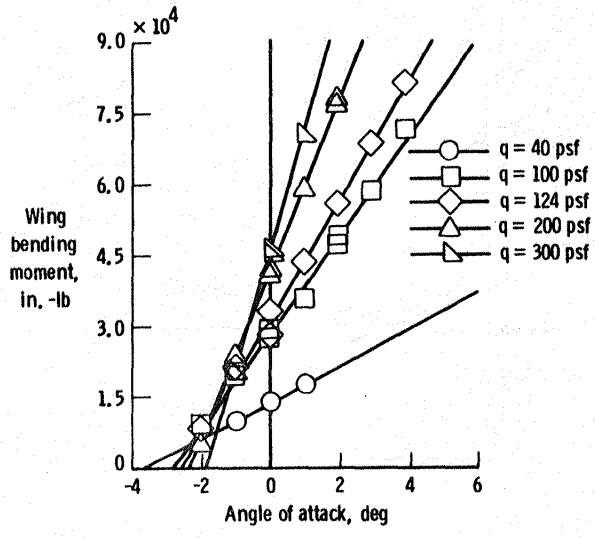

Fig. 12 Wind bending moment variation with angle of attack at five dynamic pressures; M=0.80 and δ_m=0°.

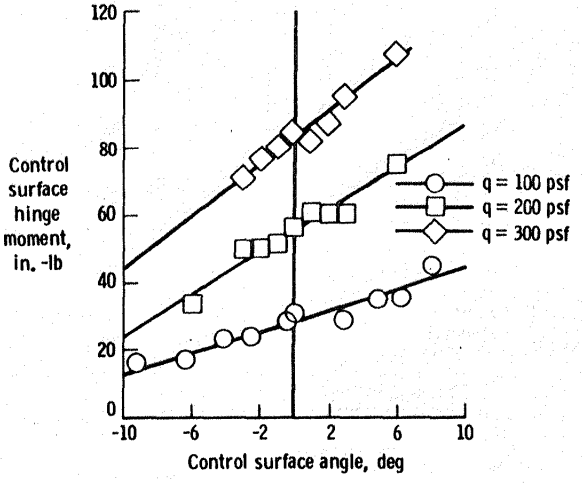

Fig. 13 Control surface hinge moment variation with control surface deflection at three dynamic pressures; M=0.80 and α=0°.

1. Report No.	2. Government Accession No.	3. Recipient's Catalog No.
NASA TM 86376		

4. Title and Subtitle	5. Report Date
MEASURED UNSTEADY TRANSONIC AERODYNAMIC CHARACTERISTICS OF AN ELASTIC SUPERCRITICAL WING WITH AN OSCILLATING CONTROL SURFACE	February 1985
	6. Performing Organization Code 505-33-43-09

7. Author(s)	8. Performing Organization Report No.
David A. Seidel, Maynard C. Sandford, and Clinton V. Eckstrom	
	10. Work Unit No.
9. Performing Organization Name and Address	
NASA Langley Research Center Hampton, VA 23665	11. Contract or Grant No.
	13. Type of Report and Period Covered
12. Sponsoring Agency Name and Address	Technical Memorandum
National Aeronautics and Space Administration Washington, DC 20546	14. Sponsoring Agency Code

15. Supplementary Notes

This paper will be presented at the AIAA/ASME/ASCE/AHS 26th Structures, Structural Dynamics and Materials Conference, Orlando, FL, April 15-17, 1985 as AIAA Paper No. 85-0598-CP.

16. Abstract

Transonic steady and unsteady aerodynamic data were measured on a large elastic wing in the NASA Langley Transonic Dynamics Tunnel. The wing had a supercritical airfoil shape and a leading-edge sweepback of 28.8°. The wing was heavily instrumented to measure both static and dynamic pressures and deflections. A hydraulically driven outboard control surface was oscillated to generate unsteady airloads on the wing. Representative results from the wind tunnel tests are presented and discussed, and the unexpected occurrence of an unusual dynamic wing instability, which was sensitive to angle of attack, is reported.

17. Key Words (Suggested by Author(s))	18. Distribution Statement
Control Surface Transonic Aerodynamics Unsteady, Steady Pressures Supercritical Wing Wind Tunnel Test DAST ARW-2	Unclassified - Unlimited Subject Category 02

19. Security Classif. (of this report)	20. Security Classif. (of this page)	21. No. of Pages	22. Price
Unclassified	Unclassified	9	A02

For sale by the National Technical Information Service, Springfield, Virginia 22161

End of Document